Remote Sensing of Environment 319 (2025) 114645

Contents lists available at ScienceDirect

Remote Sensing of Environment

journal homepage: www.elsevier.com/locate/rse

Nighttime lights reveal substantial spatial heterogeneity and inequality in post-hurricane recovery

Qiming Zheng [a,b,c,*], Yiwen Zeng [d,e], Yuyu Zhou [f], Zhuosen Wang [g,h], Te Mu [a,b,c], Qihao Weng [a,b,i,**]

[a] JC STEM Lab of Earth Observations, Department of Land Surveying and Geo-Informatics, Hong Kong Polytechnic University, Hung Hom, Kowloon, Hong Kong, Hong Kong Special Administrative Region
[b] Research Centre for Artificial Intelligence in Geomatics, The Hong Kong Polytechnic University, Hung Hom, Hong Kong, Hong Kong Special Administrative Region
[c] Department of Geography and Resource Management, The Chinese University of Hong Kong, Hong Kong, Hong Kong Special Administrative Region
[d] Asian School of the Environment and Earth Observatory of Singapore, Nanyang Technological University of Singapore, Singapore 637459, Singapore
[e] Centre for Nature-based Climate Solutions, National University of Singapore, 117546, Singapore
[f] Department of Geography, The University of Hong Kong, Hong Kong, Hong Kong Special Administrative Region
[g] Earth System Science Interdisciplinary Center, University of Maryland College Park, College Park, MD 20740, USA
[h] Terrestrial Information Systems Laboratory, NASA Goddard Space Flight Center, MD 20771, USA
[i] Research Centre for Land and Space, Hong Kong Polytechnic University, Hung Hom, Kowloon, Hong Kong, Hong Kong Special Administrative Region

ARTICLE INFO

Editor: Marie Weiss

Keywords:
Nighttime light
VIIRS
Black Marble product
Post-hurricane recovery
Inequality
FEMA

ABSTRACT

While severe hurricanes continue to challenge the resilience of local communities, fine-scale knowledge of post-hurricane recovery remains scarce. Existing recovery tracking approaches mainly rely on aggregated metrics that would disguise the spatial heterogeneity in recovery patterns. Here, we present a spatiotemporally explicit investigation into the recovery of human activity after 10 recent severe hurricanes in the U.S., with daily nighttime light (NTL) time series images from NASA's Black Marble VIIRS NTL product suite. We utilized a Bayesian-based time series change detection model and temporal clustering algorithm to analyze the post-hurricane recovery of each built-up area pixel within 446 counties severely affected by the hurricanes. To investigate the potential inaccuracies stemming from assessments using aggregated statistics, we further compared the recovery pattern estimated at pixel scale with that estimated by aggregated NTL radiance at county and census tract scales. Last, we examined the inequality in post-hurricane recovery and how it related to socioeconomic factors and current hurricane assistance programs. Our analysis shows a 7-fold difference in the recovery duration of hurricane-affected built-up areas within a county, with one-third of the areas experiencing a prolonged recovery lasting over 200 days. We emphasize the necessity of fine-scale knowledge in recovery assessments as aggregated statistics tend to largely underestimate the severity of hurricane impact and spatial heterogeneity of recovery. More importantly, we identify a prevailing recovery inequality across minority and disadvantaged populations, as well as a continued disproportionate allocation of hurricane assistance served as a key driver of exacerbating recovery inequality. Our study offers nuanced insights into the spatial heterogeneity of post-hurricane recovery that can inform strategic and equitable recovery efforts, as well as more effective hurricane relief programs and protocols.

1. Introduction

Hurricanes are among the most destructive natural disasters in the U. S. (Barton-Henry and Wenz, 2022). In the past four decades, hurricanes have inflicted approximately $1400 billion in inflation-adjusted damage, accounting for over 50 % of all damages incurred by natural disasters (Smith and Matthews, 2015). The number of severe hurricanes with damages exceeding $1 billion is also increasing, causing the total

* Corresponding author at: Department of Geography and Resource Management, The Chinese University of Hong Kong, Hong Kong, Hong Kong Special Administrative Region
** Corresponding author at: JC STEM Lab of Earth Observations, Department of Land Surveying and Geo-Informatics, Hong Kong Polytechnic University, Hung Hom, Kowloon, HHong Kong, Hong Kong Special Administrative Region.
E-mail addresses: qmzheng@cuhk.edu.hk (Q. Zheng), qihao.weng@polyu.edu.hk (Q. Weng).

https://doi.org/10.1016/j.rse.2025.114645
Received 28 December 2024; Received in revised form 30 January 2025; Accepted 3 February 2025
Available online 12 February 2025

costs of hurricane damage to surge elevenfold (NOAA, 2024). Besides direct costs, hurricanes are known to trigger a cascade of societal and ecological impacts, as well as adverse effects on physical and mental health(Andresen et al., 2023; Baade et al., 2016; Thonis et al., 2024). Given that hurricane-prone areas along the Gulf and Atlantic coasts overlap with hotspots of future population and wealth growth, the impacts of hurricanes are likely to escalate in the near future (Balaguru et al., 2023; Ohenhen et al., 2024; Wehner and Kossin, 2024).

Ensuring a timely recovery from the escalating impacts of hurricanes is therefore one of the ambitious goals for governments, as well as international initiatives such as the Sendai Framework for Disaster Risk Reduction 2015–2030 and SDGs (Target 11.5 – make human settlement resilient) (Markhvida et al., 2020). Spatiotemporally explicit information for post-hurricane recovery assessments, particularly on tracking recovery progress and its spatial pattern, is crucial for pinpointing areas in need, optimizing resource allocation, and reducing restoration costs (Sauer et al., 2023).

However, obtaining spatiotemporally explicit information on post-hurricane recovery remains challenging due to the following reasons. First, most recovery tracking methods are built upon aggregated post-hurricane statistics (e.g., at state or county scale), such as total population and electricity load (Lindell et al., 2011; Sotolongo et al., 2021), or by oversimplified approaches that compare the before-after changes of hurricanes (Chakraborty and Stokes, 2023; Zhang et al., 2023). These approaches only provide snapshots of the recovery after hurricanes, while largely overlooking the spatiotemporal heterogeneity in how neighborhoods across geographical and socioeconomic contexts respond to hurricanes differently (Jing et al., 2024). Second, recovery tracking data with large spatiotemporal availability and comparability are lacking. Power outage data, for instance, is collected under a decentralized electricity infrastructure in the U.S., comprising over 1600 utility companies with inconsistent outage reporting formats and standards (Xu et al., 2023). Other geospatial data, such as cell phone signals and point-of-interest data, offer limited spatial and temporal availability (Kerber et al., 2023). Most of the investigations using these data are constrained to a single hurricane or even a single hurricane-affected county, and their resulting conclusions are limited to be local-specific (Park et al., 2024).

These challenges have further incurred uncertainty in whether the obtained recovery information maintains fidelity across spatial scales. If not, the mismatch in spatial scale between the obtained recovery information (e.g., at state scale) and the recovery taking place (e.g., at neighborhood scale) is prone to misinterpretation of recovery progress and even worse, maladaptive interventions. Moreover, hurricanes do not equally affect neighborhoods in different socioeconomic contexts (Hong et al., 2021; Howell and Elliott, 2019; Wing et al., 2022). Despite ambitious goals and initiatives to enhance equality in disaster resilience, the lack of spatiotemporally explicit knowledge hinders investigations into hurricane recovery from the lens of environmental justice (Markhvida et al., 2020).

Nighttime light (NTL) satellite sensors are uniquely capable of detecting artificial light emitted from the Earth's surface at night (Imhoff et al., 1997; Levin et al., 2020; Shi et al., 2023). Due to a close correlation with socioeconomic variables, such as Gross Domestic Product, population density, electrification rate, and energy consumption, the detected NTL radiance has been well-documented as an ideal and integrated indicator of overall human activity intensity (Chen et al., 2019; Elvidge et al., 1997; Sánchez de Miguel et al., 2014; Zheng et al., 2022b). NTL images, such as DMSP-OLS and VIIRS, have been widely applied to quantitatively assess changes in human activity intensity incurred by natural disasters, including hurricanes (Hu et al., 2024; Levin, 2023; Román et al., 2019). Nevertheless, existing NTL-based studies mostly rely on oversimplified approaches and aggregated metrics due to the high temporal variation, noises, and missing data of daily NTL images (Mu et al., 2024; Wang et al., 2021).

In this study, we provide a spatiotemporally explicit assessment of the post-hurricane recovery of human activity using daily nighttime light images and time series modelling approaches. We aim to answer three key questions: (1) how fine-scale data can better reveal the spatiotemporal heterogeneity of post-hurricane recovery? (2) whether fine-scale knowledge is necessary for post-hurricane recovery assessment, compared with aggregated statistics? (3) whether people under different socioeconomic contexts recover at an equal rate and what are the underlying factors leading to recovery inequality? Overall, our fine-scale insights into the post-hurricane recovery pattern hold a broad scientific significance in offering data-driven knowledge to inform strategic and equitable recovery efforts, as well as more effective hurricane relief programs and protocols.

2. Study area & datasets

2.1. Study area

We focused on severe Atlantic hurricanes reaching category 4 level (max. sustained winds≥209 km per hour) and category 5 level (≥252 km per hour) in the U.S., which have received major disaster declarations from the Federal Emergency Management Agency (FEMA) and caused catastrophic impacts. Given that NASA's Black Marble VIIRS NTL product suite has only been available since 2012, we further narrowed our study objects down to 10 hurricanes, covering 7 states across the U. S. (Fig. 1). We treated each hurricane and its affected state separately as hurricane scale differs across affected states, which resulted in 17 hurricane-state pairs (e.g., Michael-Florida). For each hurricane-state pair, we only focused on the counties that were severely affected by hurricanes (n = 446), according to the "Designated Areas" (i.e., counties) defined by the corresponding disaster declaration documents of FEMA (FEMA, 2024a).

2.2. Datasets

In this study, we used the NASA's Black Marble VIIRS NTL Product Suite (VNP46A2), generated from the Visible Infrared Imaging Radiometer Suite (VIIRS) of Suomi-NPP satellite (Román et al., 2018). The Black Marble Product suite provides temporally consistent and daily NTL images at a 15-arcsec resolution (~ 500 m), an ideal spatial scale for reflecting changes at parcel level or neighborhood level (Oke et al., 2017; Zheng et al., 2022a). The Black Marble Product suite largely improves the quality of raw VIIRS NTL images via a series of routine corrections, including lunar BRDF, cloud, terrain, atmospheric, airglow, stray light, as well as a substantial sensitivity enhancement of low-lit structures (Román et al., 2018). Our analysis relied on the BRDF-corrected NTL radiance layer of VNP46A2 product. This layer of NTL image data only keeps high-quality observations, while masking out all low-quality observations, such as with cloud contamination, snow coverage, and outliers, using the Mandatory Quality Flag layer. The View Zenith Angle layer of the At-sensor TOA Nighttime Radiance data of the Black Marble Product suite (VNP46A1) were obtained for angular effect correction.

In addition to NTL images, the following datasets were obtained: (1) MODIS Land Cover Type V006 Product (MCD12Q1) (Friedl and Sulla-Menashe, 2019); (2) 11 socioeconomic variables at census tract level from the American Community Survey (ACS) via ACS API (Table S1) (Folch et al., 2016). Given that ACS are known to produce inaccurate estimates of socioeconomic variables for some census tracts, we used the ACS 5-year estimate data rather than ACS 1-year estimate data to favor accuracy over currency (Wing et al., 2022). The rationale of variable selections lies in two aspects. First, these variables are among the most commonly-used in studies assessing socioeconomic inequalities (Drakes et al., 2021; Sanders et al., 2022; Smiley et al., 2022). Second, these variables were available not only in the U.S. but also other countries, making our assessment framework easily transferable to assessing disaster recovery inequality in other countries; (3) Historical records of

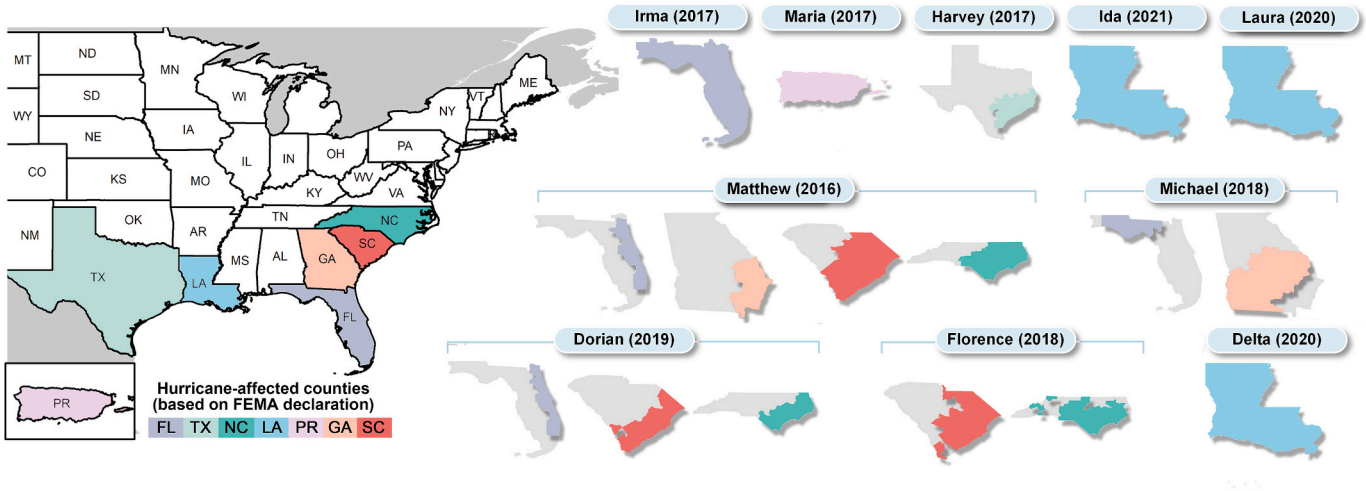

Fig. 1. The studied 17 hurricane-state pairs and the corresponding hurricane-affected counties (n = 446) based on the disaster declaration of the Federal Emergency Management Agency (FEMA).

approved FEMA assistance – via Public Assistance Program and Individuals and Households Program – of each studied hurricane via OpenFEMA database (FEMA, 2024d). Public Assistance Program (PA), FEMA's largest grant program, provides financial assistance to communities after a federally declared disaster to save lives, protect property, and restore community infrastructure. Individuals and Households Program (IHP) provides financial assistance to uninsured or underinsured individuals and households to meet their basic needs and supplement disaster recovery efforts (Emrich et al., 2022). The FEMA assistance records document detailed information about FEMA assistance approved for supporting the recovery of communities (PA) and individuals (IHP) during each hurricane, including geolocation (e.g., zip code) of assistance applicants and the amount of approved financial assistance. We calculated the total FEMA assistance received by each county and each hurricane, and inflation-adjusted total assistance to the US dollar in 2020.

3. Methods

Our analytical framework comprises three parts: (1) applying the BEAST time series modelling and change detection algorithm to the angular effect corrected nighttime light pixel time series; (2) analyzing the post-hurricane recovery pattern of hurricane-affected built-up area pixels; (3) investigating the scale effect and inequality of post-hurricane recovery. The following sections detail analysis employed in this study, together with a methodological flowchart provided in Fig. 2.

3.1. Nighttime light image pre-processing

Despite these enhancements, daily NTL images are subject to an angular effect, which has resulted in inconsistency among observations of the same location across different viewing zenith angles (VZA) (Li et al., 2022; Li et al., 2019; Tan et al., 2022). Building on the conceptual relationship identified in previous studies (Hu et al., 2024; Li et al., 2019; Xu et al., 2023), we applied a quadratic regression-based approach to convert the radiance of each pixel observation with different VZAs into the radiance at nadir observation (VZA = 0°).

$$NTL_{i,vza} = \alpha VZA_i^2 + \beta VZA_i + \varepsilon \quad (1)$$

$$f_{i,vza} = NTL_{i,vza=0} \Big/ NTL_{i,vza} \quad (2)$$

$$NTL_{i,cor} = f_{i,vza} \times NTL_{i,vza} \quad (3)$$

Where $NTL_{i,cor}$ and $NTL_{i,vza}$ refer to angular-effect-corrected and raw (with angular effect) NTL radiance of pixel i. VZA_i indicates the viewing zenith angle of pixel i; α and β are coefficients of the quadratic model.

This angular effect correction approach assumes that for a stable pixel, its NTL radiance follows a quadratic relationship against its VZA (Eq. 1). We used the NTL pixel time series during the pre-hurricane period to train a quadratic regression model (Eq. 1) and estimated the percentage difference ($f_{i,vza}$) between nadir observations ($NTL_{i,vza=0}$) and angular observations ($NTL_{i,vza}$) (Eq. 2). Then, we applied the estimated percentage difference to convert all angular observations into nadir observations (Eq. 3). Utilizing our approach, we corrected all the NTL pixel time series within our study area. We reported that on average, the angular effect contributed to an average of 5.6 % (VZA = 30°) and 10.3 % (VZA = 60°) NTL radiance bias from nadir observation (Fig. S1).

3.2. Time series modelling of daily NTL data

Here, we used a time series analysis approach to identify the pixels experiencing significant decrease in human activities (i.e., indicated by significant decrease in NTL radiance) during hurricane landfall and estimate their post-hurricane recovery patterns. We focused on built-up area pixels of hurricane-affected counties designated by FEMA (n = 446; colored areas in Fig. 1), where built-up areas were obtained from the 500-m MCD12Q1 land cover map product. However, in addition to angular effect, daily NTL data used in this study are subject to two main issues – prevailing data gaps and a large background temporal variation – that would affect the robustness of our analysis. Given that poor-quality observations (e.g., cloud contamination) had been masked out in the BRDF-corrected NTL radiance layer, there were prevailing data gaps in the daily time series. On average, these data gaps covered 30.9 %, or 113 out of 365 days, of the daily observations of each pixel. Furthermore, impacts, such as seasonality, flickering cycle and, ephemeral signals, altogether resulted in a particularly high background variations in daily NTL time series, with an average coefficient of variation of 17 % (Fig. 2) (Elvidge et al., 2022; Hsu et al., 2021; Zheng et al., 2022a).

To address these two issues, we utilized the Bayesian Estimator of Abrupt change, Seasonal change, and Trend (BEAST) model, a robust time series decomposition and change detection algorithm (Zhao et al., 2019). With an ensemble learning scheme to combine many individual models via Bayesian model averaging, the BEAST model stands out from other conventional time series models adopting a single-best-model paradigm, which is susceptible to inter-model inconsistencies against time series data with complex temporal patterns, such as daily NTL time

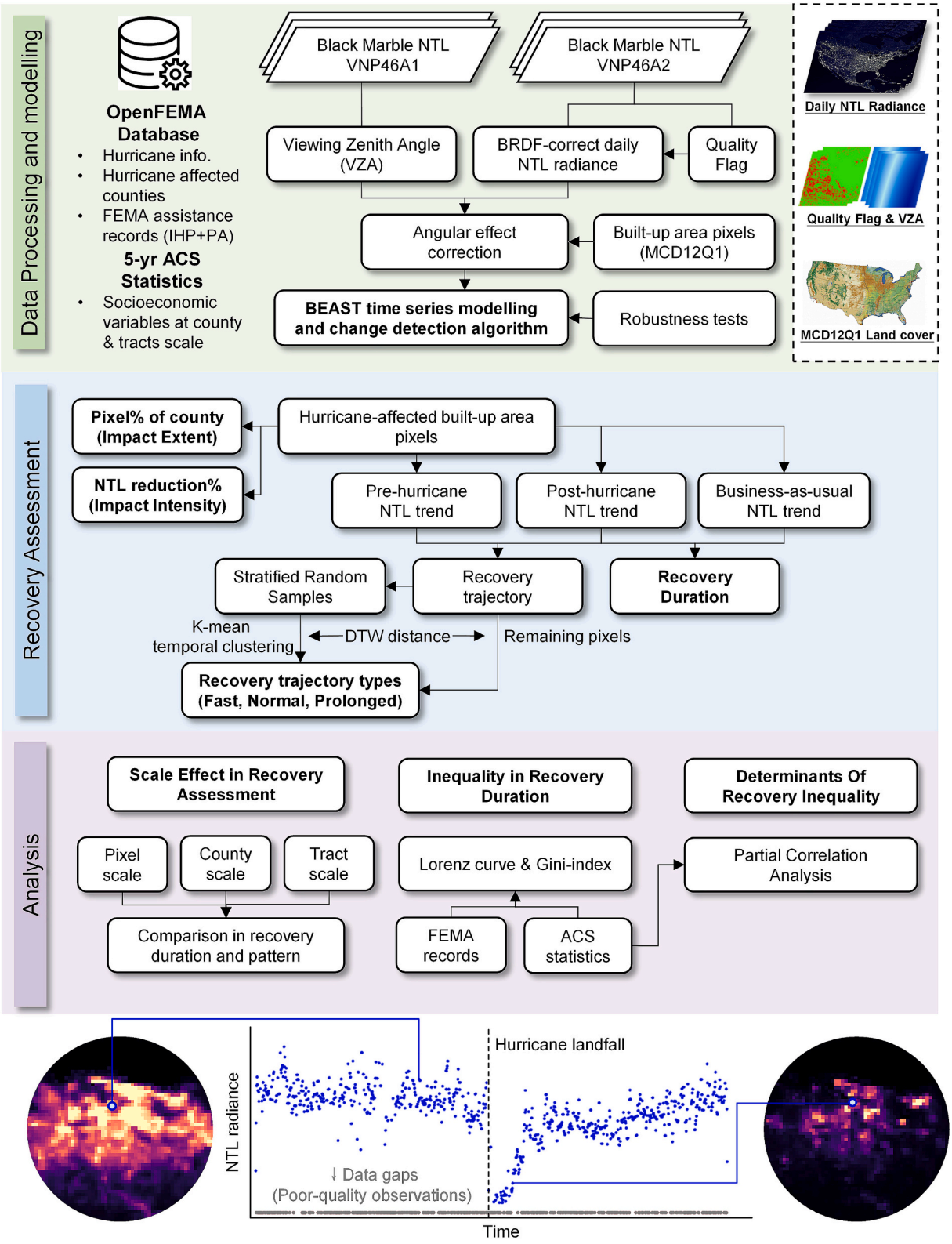

Fig. 2. Methodological flowchart of this study and the NTL time series of a typical built-up pixel of BRDF-corrected NTL radiance layer of VNP46A2 product.

series data (Wang et al., 2021; Wu and Li, 2024; Zheng et al., 2023). Moreover, the BEAST model can detect changes in irregular time series with data gaps, making it particularly suitable for the daily NTL time series used in this study.

Specifically, the BEAST model was applied to fit the daily NTL time series of each built-up pixels two years before and after the hurricane landfall. It served for two purposes: (1) to decompose the NTL time series into trend, seasonality (seasonal effect), and remainder components (other under-captured NTL variations and noises). The resulting NTL trend component – representing the response of human activity intensity to hurricane's impact – was used for the subsequent analyses; and (2) to identify built-up pixels experiencing statistically significant decrease in

NTL intensity and thus human activity intensity during hurricane landfall (hereafter referred as "hurricane-affected pixels").

We carried out a series of approaches to conservatively ensure the robustness of the detected changes; that is, the detected change should be resulted from hurricane impact and rather than the background temporal variation of daily NTL data, modelling errors, or other co-occurring events. First, the detected change must (i) fall within 15 days before and after the hurricane landfall date; (ii) have a change occurrence probability larger than 95 % - one of the output parameters of BEAST (see sensitivity analysis in Supplementary Text 1); and (iii) not be concurrent with land cover changes, such as from built-up area to non-built-up area, which is one of the key causes of significant NTL changes (Stokes and Seto, 2019; Zheng et al., 2021). Second, we calculated the deviation of observed NTL intensity to pre-hurricane NTL trend of each daily observation (ΔNTL; Eq. 4 and Fig. 3).

$$\Delta NTL_t = NTL_{pre\_trend,t} - NTL_{obs,t}$$

$$where\ NTL_{pre\_trend,t} = \begin{cases} NTL_{trend\_beast,t}, & t \in PreHurricane \\ NTL_{trend\_bau,t}, & t \in PostHurricane \end{cases} \quad (4)$$

Where t indicates the date of observation; ΔNTL stands for the deviation of observed NTL intensity (NTL_{obs}) to pre-hurricane NTL trend; the pre-hurricane NTL trend is represented by the NTL trend estimated by BEAST model (NTL_{trend_beast}) and the BAU NTL trend (NTL_{trend_bau}) during pre-hurricane period and post-hurricane period, respectively.

The ΔNTL during pre-hurricane period represent the distribution of background temporal variation of daily NTL data. If the ΔNTL during post-hurricane period ($\Delta NTL_{post,t}$) is significantly lower than the ΔNTL during pre-hurricane period ($\Delta NTL_{pre,t}$; *t*-test), it re-affirms that the detected change is caused by hurricane rather than other issues, such as background variation and modelling error (Fig. 3b).

3.3. Estimating the spatiotemporal pattern of post-hurricane recovery

With the resulting NTL trend and identified hurricane-affected built-up pixels, we quantitatively analyzed the extent and intensity of the hurricane's impacts on human activity intensity and estimated the duration of post-hurricane recovery. (1) Extent of hurricane's impact: For each hurricane-affected county, we calculated the proportion of hurricane-affected built-up areas among the total built-up areas of the county. (2) Intensity of hurricane's impact: For each hurricane-affected built-up area pixel, we measured the impact intensity by calculating the relative NTL decrease between the 180-day average NTL radiance of the pre-hurricane period and the maximum NTL radiance decrease during the hurricane landfall period. (3) Recovery duration: For each hurricane-affected built-up pixel, we estimated the recovery duration of its human activity intensity by the lapse between the timing of the detected change and the timing that the NTL trend rebounds to its business-as-usual (BAU) level. The BAU referred to a counterfactual condition that assumes the continuation of pre-hurricane condition without the influences of hurricane. The BAU NTL time series was projected by assuming a linear continuation of the NTL trend from the pre-hurricane period. By comparing the difference between BAU NTL trend (without hurricane) and observed NTL trend (human activity changes after hurricane, e.g., downturn and recovery), it allowed us to track the post-hurricane recovery trajectory and estimate the recovery duration.

To analyze the spatial heterogeneity of the post-hurricane recovery, we used a time series clustering approach to categorize the hurricane-affected built-up pixels into three recovery trajectory types based on their recovery trajectory: fast recovery, normal recovery, and prolonged recovery. Firstly, we obtained recovery trajectory by calculating the ratio between observed NTL trend and BAU NTL trend. Then, we employed a stratified sampling strategy to collect recovery trajectories of 5000 built-up pixels based on their recovery duration. Third, we used a k-mean clustering approach, with Time-Weighted Dynamic Time Warping (TWDTW) as distance measurement, to obtain three clustering centroids, representing three recovery trajectory types (i.e., fast recovery, normal recovery and prolonged recovery) (Belgiu and Csillik, 2018). For the remaining hurricane-affected built-up area pixels, we measured the distance of their recovery trajectories to the clustering centroids of each recovery trajectory type using TWDTW and assigned them to the type with the shortest distance.

We further examined how the analyses would be affected by analytical scales and whether the identified hurricane impact and recovery patterns remain fidelity across spatial scales. We aggregated the daily NTL radiance of built-up pixels and calculated the total NTL radiance of each census tract and county. Then, we applied the analyses conducted at pixel scale to the aggregated census tract scale and county scale, and compared the differences in the hurricane recovery pattern, as well as identified hurricane impacts.

3.4. Inequality of hurricane recovery and its determinants

We utilized a two-pronged approach to analyze socioeconomic inequality in post-hurricane recovery. Given that census tract is the finest spatial scale with available socioeconomic variables, we used average recovery duration of hurricane-affected pixels within a census tract to match the spatial scale of the socioeconomic variables, totaling 7175 census tracts among 17 hurricane-state pairs. We employed the Lorenz curve and Gini index to assess the inequality in recovery duration by comparing the cumulative share of recovery duration with cumulative share of variables (i.e., socioeconomic variables and received FEMA assistance) sorted in an ascending order (Sanders et al., 2022). If the recovery duration is equally distributed across these variables, the curve would distribute along the diagonal 1:1 line. Gini index gauges the

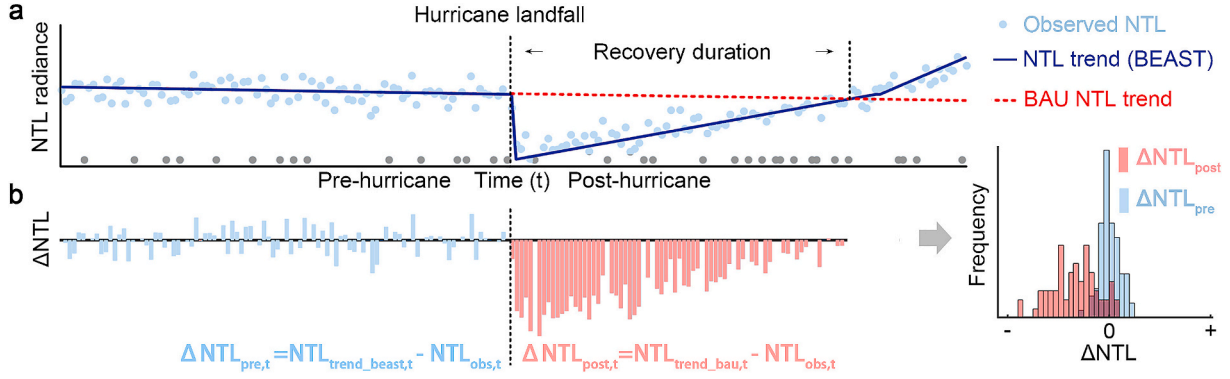

Fig. 3. Conceptual diagram of observed NTL, NTL trend estimated by BEAST model, BAU NTL trend, and recovery durations (a) and the NTL deviation to pre-hurricane NTL trend (ΔNTL; b).

extent of deviation from the equal distribution line and quantitatively measures the inequality of recovery duration distribution, ranging from 0 (equal) to -1/1 (unequal). Additionally, we used partial correlation analysis to quantify the influence of each variable to the inequality in recovery duration, while controlling the effects of other variables (e.g., hurricane intensity).

4. Results

4.1. Time series modelling

By summarizing the time series modelling performance of all the pixels, we report an average R^2 of 0.81 ± 0.14 (mean ± std) in fitting daily NTL data. Fig. 4 and Fig. S2 illustrate the modelling outcomes for

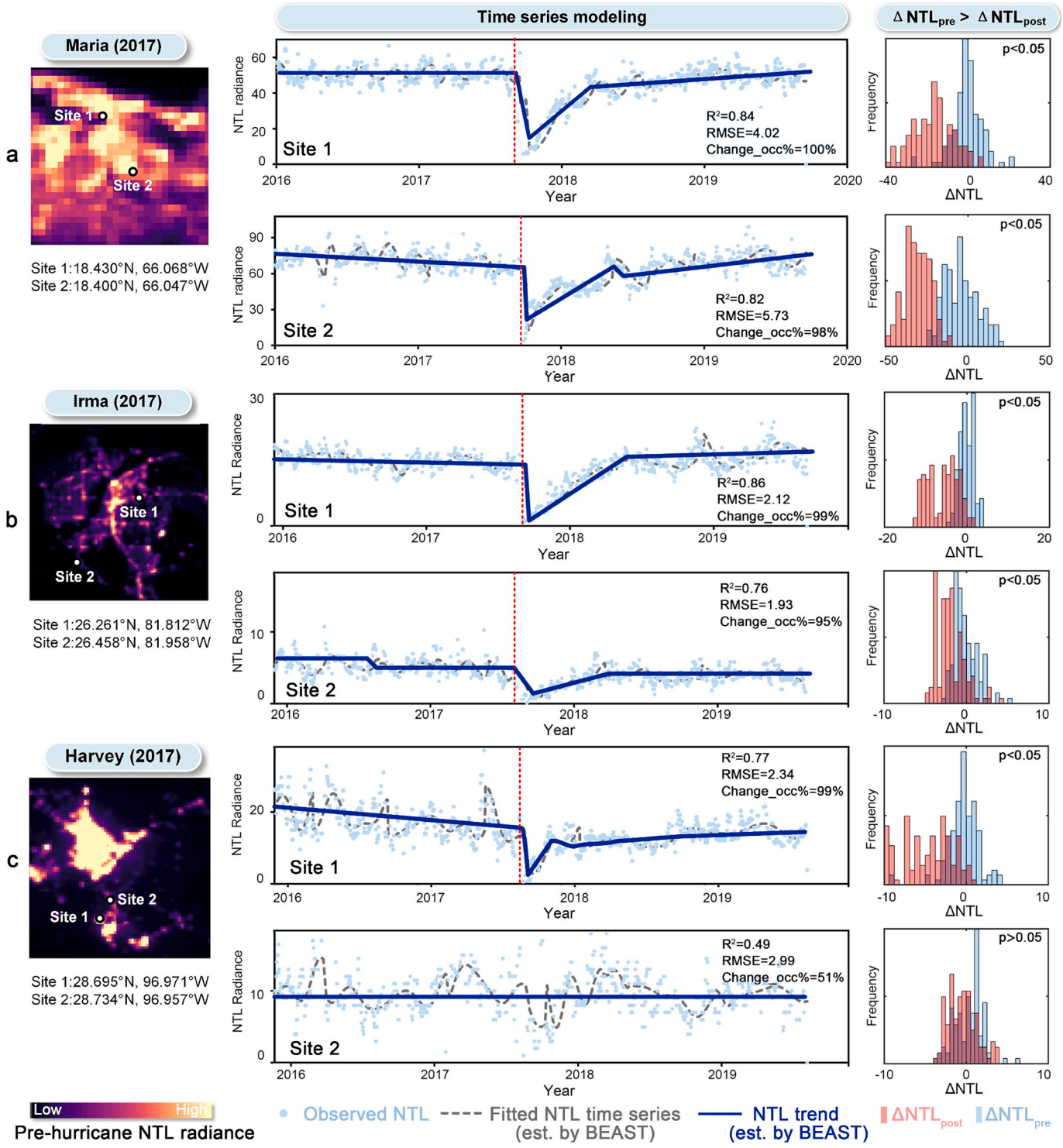

Fig. 4. Examples of BEAST time series modelling performance: Hurricane Maria (a), Hurricane Irma (b), and Hurricane Harvey (c). Left panel: NTL image; Middle panel: time series modelling performance of BEAST algorithm at two sample sites; Right panel: comparison between the NTL deviation to pre-hurricane NTL trend during pre-hurricane period ($\Delta NTL_{pre,t}$) and post-hurricane period ($\Delta NTL_{post,t}$), where the *p*-value was derived from *t*-test. Change_occ%: change occurrence probability of the detected change point.

pixels across hurricanes, locations, and NTL intensity. Our model exhibits a robust performance in detecting NTL decrease caused by hurricanes. For the pixels identified with significant NTL decrease by BEAST algorithm, 99.84 % of them show statistically significant lower ΔNTL_{post} than ΔNTL_{pre}, which re-affirms that the detected NTL decrease is resulted from hurricane rather than background temporal variation of daily NTL data or modelling errors. Nevertheless, we find that the identified hurricane-affected pixels are all with an NTL intensity approximately above 4 nW/cm^2/sr. This suggests that our model might under-detect hurricane-affect pixels in peri-urban and rural areas with low NTL intensity, as the hurricane-induced NTL decreases are likely to be buried in the high background temporal variation.

4.2. Pervasive, intense, and enduring impacts of severe hurricanes

We find that the selected hurricanes have caused pervasive and intense impacts on human activity intensity, marked by the significant decrease in NTL intensity. Figs. 5a & 5b summarize the frequency distribution of the percentage of hurricane-affected pixels of each county (Impact extent) and their corresponding NTL intensity decrease compared with the pre-hurricane level (Impact intensity) over all 17 hurricane-state pairs. Specifically, about 26 ± 24 % of the built-up pixels within each county experienced a significant decrease in NTL intensity ($p < 0.05$), and most pronounced for Hurricanes Maria (51 ± 26 %), Hurricane Matthew in Florida (32 ± 20 %), and Hurricane Michael in Florida (31 ± 21 %; Fig. 5a). For these hurricane-affected built-up pixels, we observe an average decrease of 50 ± 35 % in NTL intensity during hurricane landfall, compared with the corresponding pre-hurricane levels (Fig. 5b). Taking together, for each hurricane, approximately 19 % of the counties were severely affected, with over 50 % of built-up pixels therein experiencing at least a 75 % decrease in NTL intensity.

Our analysis shows that the pervasive and intense impacts of hurricane pose substantial challenges to a timely recovery of human activity intensity. It takes a median of 93 days (38–203 days; 25th–75th percentile, same hereinafter) for hurricane-affected built-up areas to recover to BAU level (Fig. 5c). Our estimated recovery duration at pixel scale are in accordance with the electricity restoration statistics from US Department of Energy (U.S. DOE, 2018) (Pearson correlation coefficient = 0.86), while direct comparison is not possible since different hurricane assessment indicators are used (Fig. S3). Besides, the estimated recovery duration and patterns are consistent with previous case studies looking into a single hurricane at different spatial scales (Chakraborty and Stokes, 2023; Friedrich et al., 2024; Jia et al., 2023; Park et al., 2024; Román et al., 2019). In addition, despite different socioeconomic conditions and coping capabilities from other states of the conterminous the U.S. (Dietz, 2018), our further analysis indicates the inclusion of Hurricane Maria would not significantly bias the overall recovery duration statistics (Supplementary Text S2).

We observe significant heterogeneity in the recovery duration within a county. For hurricane-affected built-up area pixels within a county, there is an average of 7-fold differences in the recovery duration between the higher 75th percentile and the lower 25th percentile (Fig. 5d). Comparing the recovery duration of built-up pixels in urban and rural areas within each county ($n = 446$), however, built-up pixels in urban areas and rural areas share a similar recovery duration without statistically significant difference for most counties ($p > 0.05$; 73 %). Built-up pixels in rural areas exhibit longer recovery durations than those in urban areas for 20 % of the counties, suggesting the rural areas in these counties are less resilient to hurricane impacts (Fig. S4).

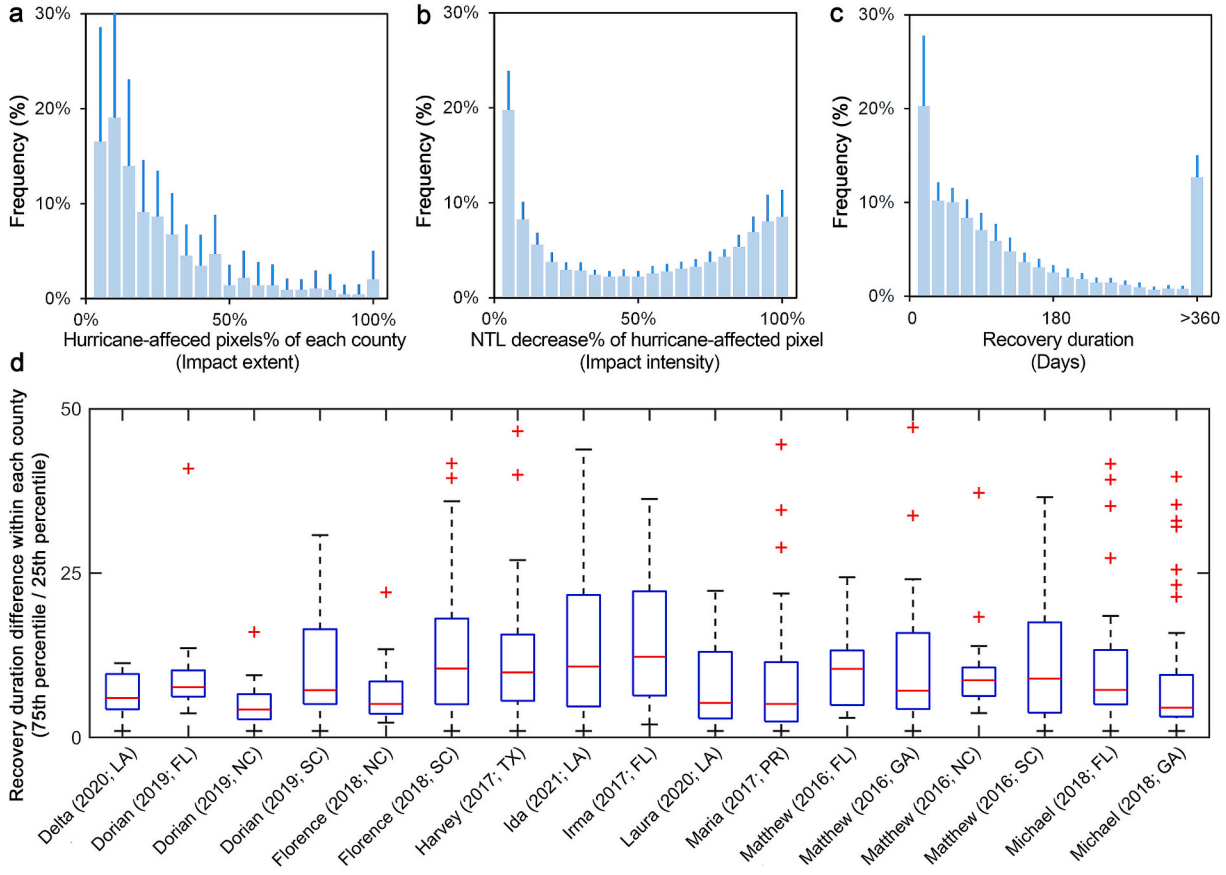

Fig. 5. Impacts of severe hurricanes. (a) Extent of hurricane impact (percentage of hurricane-affected built-up pixels of each county); (b) Intensity of hurricane impact (NTL decrease compared with pre-hurricane level); (c) Recovery duration. Each bar and error stick present the mean and standard deviation value across all hurricane-state pairs; (d) Recovery duration differences within each county (75th percentile / 25th percentile).

Our temporal clustering analysis reveals that the majority (48 %) of the built-up areas recover to their BAU level of human activity intensity in a median of 68 days (49–89 days; normal recovery), while 24 % of the built-up areas only take less than 19 days (13–25 days) to return to BAU level (fast recovery) (Fig. 6a). However, a considerable portion of built-up areas (28 %) undergo a prolonged recovery lasting for 205 days (150–299 days), which triples the median recovery duration of those with a normal recovery trajectory. Among the built-up areas experiencing a prolonged recovery, 42 % fail to recover to their BAU level of human activity intensity even 12 months after the hurricane landfall. Our wall-to-wall maps provide insights into the spatial distribution of built-up areas experiencing prolonged recovery within a county (Figs. 6b & 6c; more examples in Fig. S5).

4.3. Needs for spatiotemporally explicit information in hurricane recovery assessment

Applying our method at pixel scale to census tract scale and county scale using the aggregated total NTL intensity of all built-up pixels therein and comparing the resulting recovery patterns, we find that spatiotemporally explicit information is imperative for accurately assessing post-hurricane recovery (Fig. 7). The recovery patterns estimated at the pixel, county and census tracts scales vary greatly and relying on aggregated statistics tends to misinterpret recovery conditions. Our estimates at county and census tract scales show that 94 % of the counties and 60 % of the census tracts experience statistically significant decrease in human activity intensity upon hurricane landfall (Fig. 7a). Among these counties and census tracts, however, an average of 92 % and 59 % of hurricane-affected built-up area pixels therein exhibit a longer recovery duration than their corresponding county and census tract, respectively (Fig. 7b). This finding suggests that when the aggregated NTL radiance indicates a county or census tract has recovered to its BAU level, a considerable portion of hurricane-affected built-up area pixels therein actually remains unrecovered. On average, 40 % and 36 % of hurricane-affected built-up area pixels only recover to less than half of their BAU level, respectively, even when their corresponding counties and census tracts indicate to have fully recovered (Fig. 7c). These figures can go up to 66 % at county scale (Hurricane Maria) and 46 % at census tract scale (Hurricane Harvey). Furthermore, built-up areas experiencing a prolonged recovery trajectory are prone to be underestimated and buried in assessments using aggregated statistics. While pixel-scale analysis reports that nearly 30 % of the hurricane-affected built-up areas suffer from a prolonged recovery, it becomes less prevailing when being analyzed from census tract (14 %) and county (9 %) scales (Fig. S6).

Comparison among the recovery patterns estimated by NTL time series of hurricane-affected built-up pixels (pixel scale), aggregated NTL time series (county scale), and electricity restoration statistics (state scale) (U.S. DOE, 2018) further corroborates our finding on the scale dependency of recovery assessments. The recovery duration estimated at pixel scale is 36 days (17–72 days) and 61 days (33–83 days) longer than that estimated at county scale and state scale, respectively (Fig. S2). In fact, analysis at census tract and county scale may also under-detect the extent of hurricane-affected areas and the intensity of hurricane impacts (Supplementary Text S3).

4.4. Inequality in post-hurricane recovery and its determinant

The Lorenz curves and Gini index (G) of all 17 hurricane-state pairs indicate a noticeable inequality in the recovery duration across different socioeconomic contexts (hereafter referred as “recovery inequality”). Hispanic population (G = 0.52) and non-Hispanic Black population (G = 0.65) tend to experience an overwhelmingly longer recovery duration than other ethnic groups (Figs. 8b & 8c). On average, census tracts with Hispanic and non-Hispanic Black populations greater than 50th percentile contribute 88 % and 90 % of the cumulative share of recovery duration, respectively. In contrast, populations with a larger share of non-Hispanic White population, a higher household income, and a larger amount of received disaster assistance from the Federal Emergency Management Agency (FEMA) show a disproportionately shorter recovery duration (Figs. 8e-8g). Taking Hurricane Michael in Georgia as an example, the median recovery duration of the populations with household incomes above the 50th percentile is 16-day shorter than their counterparts. Despite the prevailing inequality across most socioeconomic variables, we observe minor recovery inequality over property value (G = -0.08) and the share of non-Hispanic Asian population (G = 0.10), whose Lorenz curves indicate no statistical significance in deviating from the 1:1 equal distribution line ($p > 0.05$; Figs. 8d & 8h).

Outcomes of partial correlation analysis corroborate the close association between recovery inequality and socioeconomic factors (Fig. 9). Census tracts with large proportion of Non-Hispanic Black population ($r = 0.50 \pm 0.16$; 95 % CI), White population ($r = 0.32 \pm 0.21$), and Hispanic population ($r = 0.20 \pm 0.18$) are vulnerable to recovery inequality, underscoring disparities in coping capabilities of severe hurricanes across races and ethnic groups. Under-education rates (i.e., with a high school diploma and below) and unemployment rates also play a significant role in worsening recovery inequality. Surprisingly, while FEMA assistance is designed to expedite post-hurricane recovery, we observe a notable inequality in FEMA assistance allocation (hereafter referred as “FEMA allocation inequality”; G = 0.59), which serves as a key contributing factor to the recovery inequality ($r = 0.65 \pm 0.35$; $p < 0.05$). Besides, there is a statistically significant increasing trend in the FEMA allocation inequality, which would very likely continue to exacerbate the recovery inequality in future hurricanes (Fig. S7). The amount of received FEMA assistance ($r = 0.14 \pm 0.13$; $p < 0.05$) and whether FEMA assistance is provided ($r = 0.06 \pm 0.26$; $p > 0.05$), however, only play a marginal role in recovery inequality, respectively.

5. Discussions

5.1. Advantages of NTL-based Post-hurricane recovery assessment

Our proposed framework re-affirms and further expand the capability of daily NTL time series data as a feasible solution to effective post-hurricane recovery assessment. It advances traditional approaches in the following aspects. First, daily NTL time series provide temporally consistent and near real-time estimation of post-hurricane recovery, which largely addresses the inconsistency and temporal lagging issues in traditional approaches. Taking Hurricane Maria as an example, the official weekly hurricane recovery reports from the US Department of Energy first adopted the electricity load as a rough proxy of customers with power when the actual statistics were not available in the first two months (Period 1 in Fig. 10) (U.S. DOE, 2018). Estimates of power restoration of customers were only available four months after the hurricane landfall (Period 3 in Fig. 10). Even so, the customers with power might not accurately represent the population with power as customers are typically defined by an electric meter, a building, or a facility (Brelsford et al., 2024).

Second, given that the daily NTL images are continuously updating and freely accessible globally, our framework holds a promising potential to be adapted for other regions and disasters (e.g., floods, winter storms, and earthquakes) with minor adjustments and additional sensitivity analyses. For many developing countries, particularly, effective disaster recovery tracking are still unavailable or simply relying on bottom-up indicators such as utility records, population statistics, and self-reporting data (Farquharson et al., 2018). For example, a recent study of 109 developing countries indicated that utility records only report 15 % of customer-reported extent of power outages (Correa et al., 2018). The use of daily NTL images, coupled with geospatial and time series modelling approaches, will bring tangible benefits to improve these countries’ disaster recovery assessment capability at a minimal cost. Third and most importantly, the fine-scale insights into

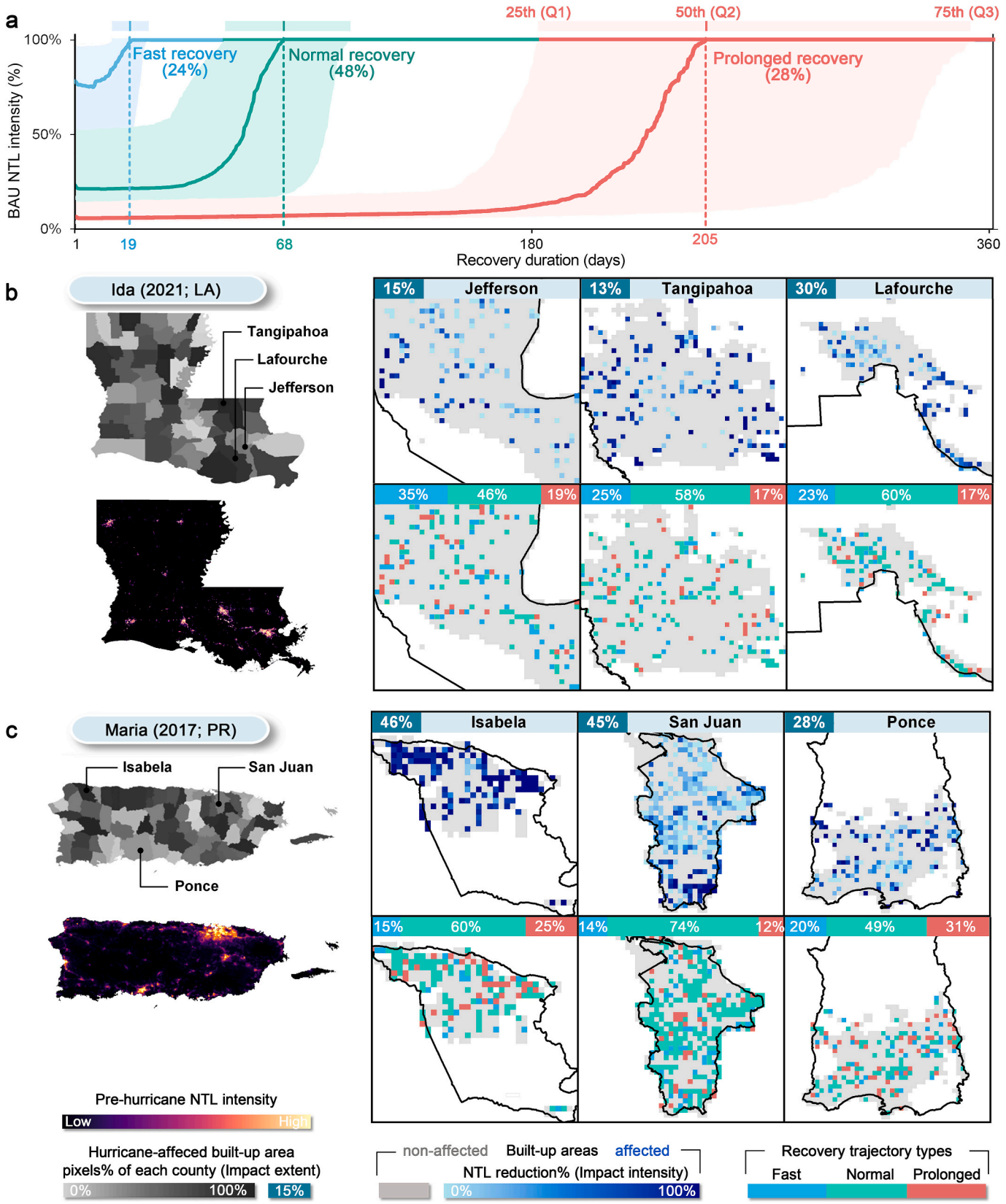

Fig. 6. (a) Temporally clustered recovery trajectory types: The dark lines indicate the median of each recovery trajectory cluster, while the shaded areas present the 25th and 75th percentile of each cluster. (b-c) Two cases of our identified the impacts and recovery patterns: Hurricane Ida and Hurricane Maria.

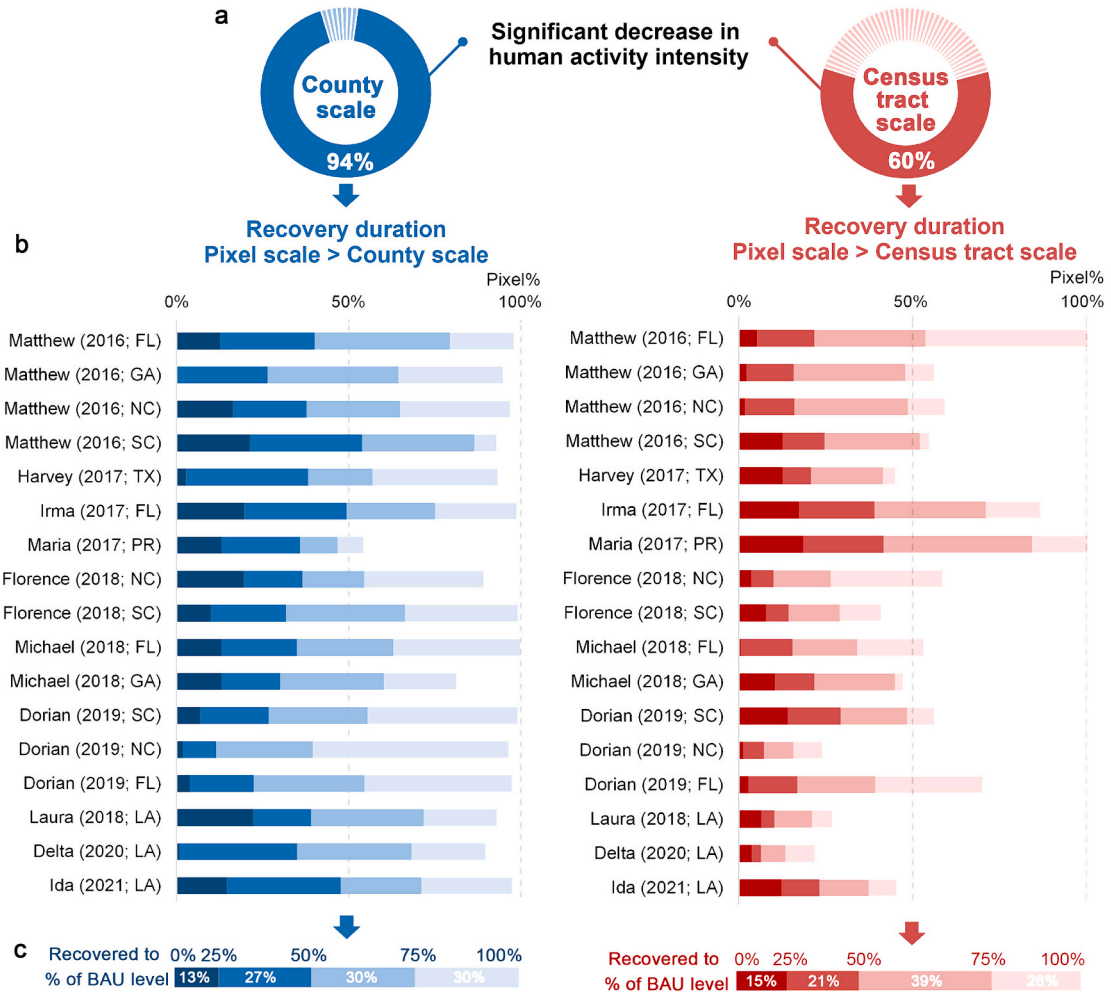

Fig. 7. Impact of analytical scale on the estimated recovery pattern. (a) Percentage of counties and census tracts showing a statistically significant decrease in human activity intensity, as detected by the aggregated total NTL radiance of each county and census tract. (b) Comparison between the recovery duration of pixel scale and aggregated scale (i.e., county scale and census tract scale): Percentage of hurricane-affected built-up pixels (estimated at pixel scale), whose recovery duration is longer than its corresponding county or census tract (estimated at aggregated scales). The color scale indicates the proportion of pixels that recover to different degrees of BAU level when their corresponding county or census tract is fully recovered. (c) Average pixel-scale recovery condition of selected hurricanes.

recovery duration patterns deliver a series of implications essential to support effective post-hurricane recovery (see detailed discussions below).

5.2. *Implication to a better Post-hurricane recovery*

The identified large difference in the recovery duration of pixels across space and hurricanes highlights the importance of understanding the spatiotemporal heterogeneity of post-hurricane recovery. It offers guidance on where decision-makers, emergency management agencies, and insurance companies should strategically prioritize their restoration efforts. Our identified built-up areas experiencing a prolonged recovery enable decision-makers to pinpoint the locations most in need of prioritized assistance on a sub-county or sub-census tract scale, which are unattainable from traditional recovery tracking approaches relying on aggregated statistics (Figs. 7b & 7c). This is crucial to mitigating the socioeconomic consequences of failure to speed up recovery, such as morbidity and mortality, displacement, social segregation, and bankruptcy (Billings et al., 2022; Fussell et al., 2010; Parks et al., 2022). Besides, a spatiotemporally explicit understanding of recovery patterns can help to shift the widely adopted density-based hurricane restoration protocols – prioritizing densely populated urban areas that tend to disadvantage vulnerable populations in rural and detached communities – to evidence-based protocols and better balance trade-offs between densely populated communities and vulnerable communities (Khan et al., 2018; Park et al., 2024). Last, our analysis indicates estimation of post-hurricane recovery is heavily scale dependent. Aggregated statistics or data with very coarse spatial resolutions (e.g., >10 km) should be used with caution for informing post-hurricane recovery. Using aggregated statistics or coarse-resolution data will risk disguising considerable heterogeneity and overlooking the neighborhoods struggling in recovery, consequently leading to maladaptation outcomes. Thus, it is of urgent necessity for future post-hurricane assessments to incorporate fine-scale information, at least as a complement, with other approaches to obtain a more comprehensive understanding on the recovery progress.

Spatiotemporally explicit understanding of hurricane recovery also facilitates decision-makers in identifying possible solutions to reduce recovery inequality in the future. Our analysis suggests that rates of recovery are highly dependent on the ethnic makeup and education level of an area, suggesting a compounding impact of natural disasters on disadvantaged communities. This corroborates existing arguments that communities with better education are often more informed, risk-aware, and resilient, thereby better equipped to adapt and respond to severe hurricanes (Brelsford et al., 2024; Gould et al., 2024; Ronco et al., 2023). It also implies that the language barrier and complexity of

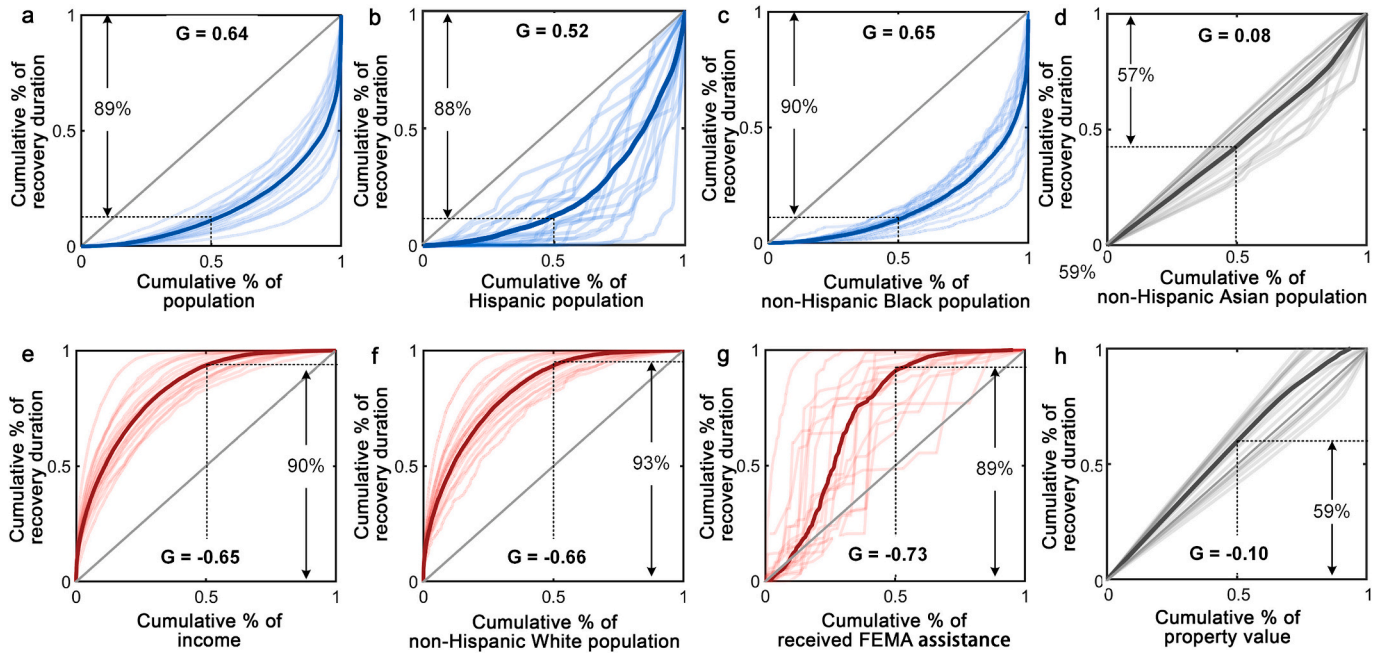

Fig. 8. The inequality measurement of hurricane recovery duration. (a-h), Lorenz curve and Gini index (G) of recovery duration over socioeconomic variables. The dark lines indicate the median of the Lorenz curve of all 17 hurricane-state pairs (light lines).

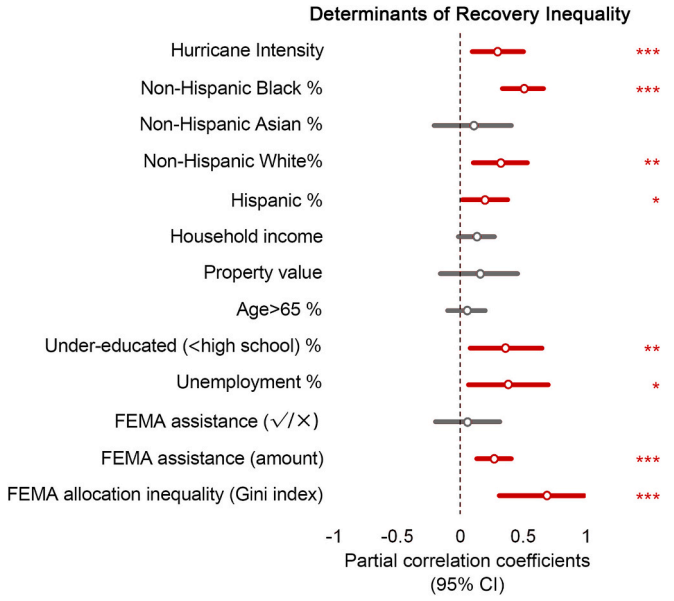

Fig. 9. Partial correlation coefficients of the driving factors for recovery inequality. Results are summarized from 17 hurricane-state combinations (*: $p < 0.05$; **: $p < 0.01$; ***: $p < 0.001$).

assistance application procedure can hinder disadvantaged communities from obtaining support for recovery (Li et al., 2023). As one of the largest expenditures of disaster relief programs, one of FEMA's ongoing endeavors is to "break down barriers and ensure an equal disaster recovery" (FEMA, 2024b). However, our findings suggest that the FEMA assistance allocation, in fact, exacerbates the inequality of hurricane recovery. This finding echoes a growing body of evidence and sentiment that the federal disaster program lacks the ability to effectively reduce the financial burden of natural disasters for many who need it urgently, particularly for minorities and disadvantaged populations. Unfortunately, this adverse influence is expected to continue and even escalate due to the regression trend in the amount of FEMA assistance provided per application and its allocation equality (Billings et al., 2022). One recent study found a three-time higher denial rate for neighborhoods with high Black people share than those with high White people share, which accounts for the falling approval rate of FEMA individual assistance program (Vestby et al., 2024). These shreds of findings emphasize that it is insufficient to provide disaster recovery assistance for effective hurricane recovery, and highlights the urgent need for FEMA to enhance its allocation equality, such as via an improved application and review procedure, providing targeted assistance to disadvantaged groups (e.g., the under-educated and unemployed).

At a broader scale, our findings hold significance for buttressing and improving initiatives aimed at reducing risks and enhancing resilience of disasters, such as the 2022–2026 FEMA Strategic Plan (Goal 1 - instill equity) (FEMA, 2023, 2024c), the Sendai Framework for Disaster Risk Reduction (Aitsi-Selmi et al., 2015; Markhvida et al., 2020), and SDGs (Target 11.5 - make human settlements resilient and Target 10.4 – achieve great equality) (Griggs et al., 2013). For example, our findings necessitate the following essential improvements in the current 38 assessment indicators for measuring the implementation progress of Sendai Framework Disaster Risk Reduction: (1) including recovery assessment indicators in addition to indicators assessing disaster impacts (e.g., loss and damage); (2) adding a sub-set of assessment indicators looking into the equality in disaster risk reduction, which is absent in the current indicator set. In fact, such improvement was also suggested by a recent review report from the United Nations (UN, 2023); (3) developing disaggregated assessment indicators: many Sendai Framework indicators are assessed at a per 100,000 people basis, which approximately is four-time of median population size of a county in the U.S. (25,950 as of 2023) (United States Census Bureau, 2023). Disaggregated indicators accounting for local conditions at sub-county or sub-census tract scale are necessary for accurate disaster risk assessment without overlooking spatial heterogeneity in the impact and recovery of disaster.

5.3. Limitations and uncertainties

It is important to acknowledge several constraints and limitations in our study. Firstly, we treated and tracked the impact of each hurricane separately, which may have underestimated the cumulative impact in

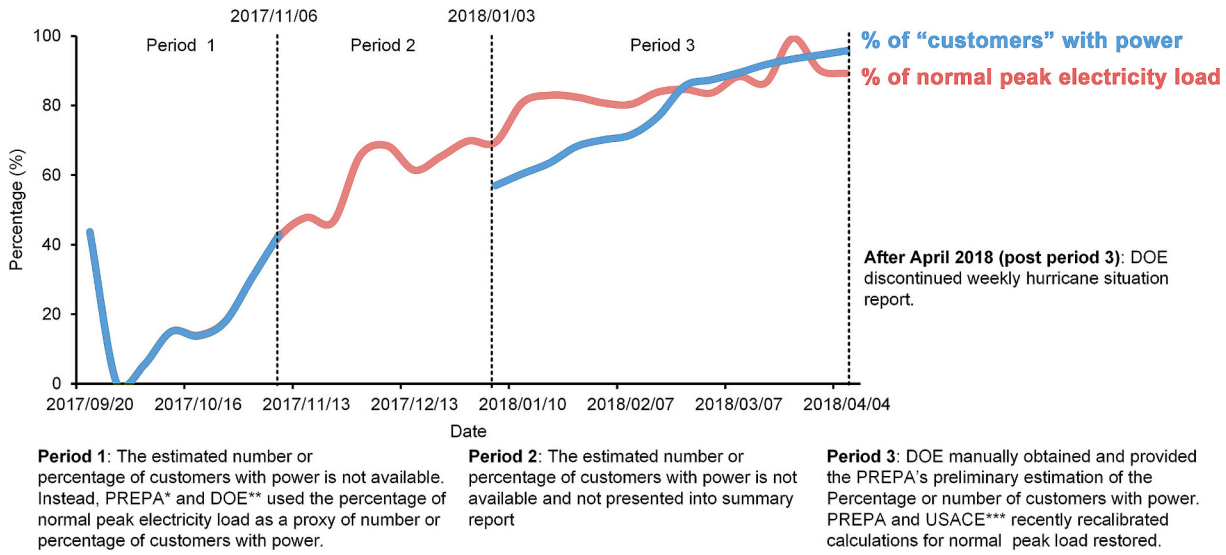

Fig. 10. Hurricane recovery status is presented by two sources of official statistics: the percentage of the normal peak electricity load of pre-hurricane period and the percentage of population with power (restored) compared with pre-hurricane period. Note: *PREPA: The Puerto Rico Electric Power Authority; **DOE: Department of Energy; *** USACE: U.S. Army Corps of Engineers.

cases where consecutive hurricanes strike the same location in quick succession (Machlis et al., 2022). An example is Hurricane Laura (Aug. 26, 2020) and Hurricane Delta (Oct. 6, 2020), both affecting Louisiana in 2020. Upon the landfall of Hurricane Delta, about 38 % of the built-up pixels affected by Hurricane Laura have fully recovered to BAU level, while 12 % only recovered to less than 25 % of their BAU level. Despite a low occurrence rate of sequential hurricanes in the past decades, the chance of sequential hurricanes is projected to increase sharply under median/high emission future development scenarios (Xi et al., 2023). Secondly, while the capability of indicating human activities changes of VIIRS NTL data has been well-acknowledged, its inherent limitations would introduce uncertainties into our analysis, including the impacts of overpass time (Li et al., 2020), flicker cycle (Elvidge et al., 2022), data gaps (Zheng et al., 2022a), and spectral setting (Kyba et al., 2014). For example, the overpass time of VIIRS NTL data is about 1:30 am (local time), during which many outdoor lighting facilities are turned off (Elvidge et al., 2013). Our simplified sensitivity analysis indicates that the off-peak overpass time of VIIRS is likely to underestimate spatial heterogeneity in the identified recovery duration and recovery inequality (Supplementary Text S4). While the BEAST model can fit time series with data gaps, our sensitivity analysis indicates that the data gaps during hurricane landfall period would underestimate the hurricane impact intensity by approximately 7 % and slightly overestimate recovery duration by 3 % (Supplementary Text S5). Despite these limitations, VIIRS thus far remains as the only NTL data with a global and long-term data coverage, free accessibility, and radiometrically calibrated NTL intensity. New NTL data, such as SDGSAT-1, might open new opportunities for an improved representation of human activities, but the validity requires further scrutiny (Jia et al., 2024). Thirdly, while NTL data closely correlate with socioeconomic activities, they only serve as a general proxy for human activity intensity and its changes, omitting recovery in other dimensions such as physical and mental well-being, supply chains, and regional economic linkage, etc. (Kim and Bui, 2019). Besides, recovery inequality may be associated with several other factors that were not measured directly or not available for our analysis (e.g., hurricane insurance, building materials, and greenspace configuration). Further investigations into these dimensions are expected to better inform post-hurricane recovery efforts.

6. Conclusions

The increasing frequency and severity of hurricanes along the U.S. Gulf and East coasts, coupled with the projected population and economic growth therein, are anticipated to pose challenges to socioeconomic recovery from hurricanes. This study illustrates the benefits of utilizing NTL imagery and time series modelling to derive spatiotemporally explicit measures of post-hurricane recovery. Our findings suggest a large spatial heterogeneity in recovery duration, which is prone to be underestimated when aggregated statistics are used in recovery assessments. Also, we identify substantial inequality in recovery across racial and disadvantaged groups, with current disaster relief programs exacerbating the issue. Nuances derived from such fine-scale analyses are necessary for countries to develop a precise and equitable hurricane recovery strategy and improve current disaster restoration and assistance protocols.

We highlight the necessities of following improvements and investigations in future studies: (1) to translate NTL-based recovery knowledge into actionable information that can be easily interpreted and applied by non-technical stakeholders (e.g., first-responders of hurricanes and rescue resource allocators), as well as poorly equipped developing countries; (2) to calibrate and improve top-down recovery tracking approaches (e.g., our NTL-based method) with bottom-up datasets, such as customer reports and utility companies (e.g., a recent data product from (Brelsford et al., 2024)); (3) to examine the performance of our method in tracking the recovery of other disasters; and (4) to better quantify the uncertainties and disentangle the noises of daily NTL data.

CRediT authorship contribution statement

Qiming Zheng: Writing – review & editing, Writing – original draft, Visualization, Validation, Methodology, Funding acquisition, Formal analysis, Data curation, Conceptualization. **Yiwen Zeng:** Writing – review & editing, Writing – original draft, Conceptualization. **Yuyu Zhou:** Writing – review & editing, Writing – original draft, Conceptualization. **Zhuosen Wang:** Writing – review & editing, Writing – original draft, Conceptualization. **Te Mu:** Writing – review & editing, Writing – original draft, Formal analysis. **Qihao Weng:** Writing – review & editing, Writing – original draft, Funding acquisition, Conceptualization.

Declaration of competing interest

All the authors declare no competing interests.

Acknowledgments

Qiming Zheng is supported by the Chinese University of Hong Kong (4937239) and General Research Fund of Research Grants Council (CUHK, 15204824). Qihao Weng is supported by Global STEM Professorship by the Hong Kong SAR Government (P0039329) and Hong Kong Polytechnic University (P0046482, P0038446, and P0042484).

Appendix A. Supplementary data

Supplementary data to this article can be found online at https://doi.org/10.1016/j.rse.2025.114645.

Data availability

Data will be made available on request.

References

Aitsi-Selmi, A., Egawa, S., Sasaki, H., Wannous, C., Murray, V., 2015. The Sendai framework for disaster risk reduction: renewing the global commitment to people's resilience, health, and well-being. Int. J. Disaster Risk Sci. 6, 164–176.

Andresen, A.X., Kurtz, L.C., Hondula, D.M., Meerow, S., Gall, M., 2023. Understanding the social impacts of power outages in North America: a systematic review. Environ. Res. Lett. 18 (5). https://doi.org/10.1088/1748-9326/acc7b9.

Baade, R.A., Baumann, R., Matheson, V., 2016. Estimating the economic impact of natural and social disasters, with an application to hurricane Katrina. Urban Stud. 44 (11), 2061–2076. https://doi.org/10.1080/00420980701518917.

Balaguru, K., Xu, W., Chang, C.C., Leung, L.R., Judi, D.R., Hagos, S., et al., 2023. Increased U.S. coastal hurricane risk under climate change. Sci. Adv. 9 (14), eadf0259. https://doi.org/10.1126/sciadv.adf0259.

Barton-Henry, K., Wenz, L., 2022. Nighttime light data reveal lack of full recovery after hurricanes in southern US. Environ. Res. Lett. 17 (11). https://doi.org/10.1088/1748-9326/ac998d.

Belgiu, M., Csillik, O., 2018. Sentinel-2 cropland mapping using pixel-based and object-based time-weighted dynamic time warping analysis. Remote Sens. Environ. 204, 509–523. https://doi.org/10.1016/j.rse.2017.10.005.

Billings, S.B., Gallagher, E.A., Ricketts, L., 2022. Let the rich be flooded: the distribution of financial aid and distress after hurricane harvey. J. Financ. Econ. 146 (2), 797–819. https://doi.org/10.1016/j.jfineco.2021.11.006.

Brelsford, C., Tennille, S., Myers, A., Chinthavali, S., Tansakul, V., Denman, M.,… Bhaduri, B., 2024. A dataset of recorded electricity outages by United States county 2014-2022. Sci. Data 11 (1), 271. https://doi.org/10.1038/s41597-024-03095-5.

Chakraborty, S., Stokes, E.C., 2023. Adaptive modeling of satellite-derived nighttime lights time-series for tracking urban change processes using machine learning. Remote Sens. Environ. 298. https://doi.org/10.1016/j.rse.2023.113818.

Chen, Z.Q., Yu, B.L., Ta, N., Shi, K.F., Yang, C.S., Wang, C., et al., 2019. Delineating seasonal relationships between Suomi NPP-VIIRS nighttime light and human activity across Shanghai, China. IEEE J. Select. Top. Appl Earth Observ. Remote Sens. 12 (11), 4275–4283. https://doi.org/10.1109/Jstars.2019.2916323.

Correa, S., Klugman, N., Taneja, J., 2018. How many smartphones does it take to detect a power outage?. In: Proceedings of the Ninth International Conference on Future Energy Systems.

Dietz, J.L., 2018. Economic History of Puerto Rico: Institutional Change and Capitalist Development.

Drakes, O., Tate, E., Rainey, J., Brody, S., 2021. Social vulnerability and short-term disaster assistance in the United States. In. J. Disaster Risk Reduct. 53. https://doi.org/10.1016/j.ijdrr.2020.102010.

Elvidge, C., Baugh, K., Kihn, E.A., Kroehl, H.W., Davis, E.R., Davis, C.W., 1997. Relation between satellite observed visible-near infrared emissions, population, economic activity and electric power consumption. Int. J. Remote Sens. 18 (6), 1373–1379. https://doi.org/10.1080/014311697218485.

Elvidge, C., Baugh, K., Zhizhin, M., Hsu, F.-C., 2013. Why VIIRS data are superior to DMSP for mapping nighttime lights. Proc. Asia Pacific Adv. Network 35 (0), 62. https://doi.org/10.7125/apan.35.7.

Elvidge, C.D., Zhizhin, M., Keith, D., Miller, S.D., Hsu, F.C., Ghosh, T., et al., 2022. The VIIRS day/night band: A flicker meter in space? Remote Sens. 14 (6). https://doi.org/10.3390/rs14061316.

Emrich, C.T., Aksha, S.K., Zhou, Y., 2022. Assessing distributive inequities in FEMA's disaster recovery assistance fund allocation. In. J. Disaster Risk Reduct. 74. https://doi.org/10.1016/j.ijdrr.2022.102855 https://doi.org/ARTN 102855.

Farquharson, D., Jaramillo, P., Samaras, C., 2018. Sustainability implications of electricity outages in sub-Saharan Africa. Nat. Sustain. 1 (10), 589–597. https://doi.org/10.1038/s41893-018-0151-8.

FEMA, 2023. Achieving Equitable Recovery A Post-Disaster Guide for Local Officials and Leaders. https://www.fema.gov/sites/default/files/documents/fema_equitable-recovery-post-disaster-guide-local-officials-leaders.pdf.

FEMA, 2024a. Disasters and Other Declarations. https://www.fema.gov/disaster/declarations?field_dv2_declaration_date_value%5Bmin%5D=2019&field_dv2_declaration_date_value%5Bmax%5D=2019&field_dv2_declaration_type_value=DR&field_dv2_incident_type_target_id_selective=49124.

FEMA, 2024b. FEMA Offers Equal Access to All Disaster Survivors. https://www.fema.gov/fact-sheet/fema-offers-equal-access-all-disaster-survivors.

FEMA, 2024c. FEMA Strategic Plan. Retrieved Mar 1, 2024 from. https://www.fema.gov/about/strategic-plan.

FEMA, 2024d. OpenFEMA Data Sets. Retrieved 2024-04-01 from. https://www.fema.gov/about/openfema/data-sets#public.

Folch, D.C., Arribas-Bel, D., Koschinsky, J., Spielman, S.E., 2016. Spatial variation in the quality of American community survey estimates. Demography 53 (5), 1535–1554.

Friedl, M., Sulla-Menashe, D., 2019. MODIS/Terra+Aqua Land Cover Type Yearly L3 Global 500m SIN Grid V006. https://doi.org/10.5067/MODIS/MCD12Q1.006.

Friedrich, H.K., Tellman, B., Sullivan, J.A., Saunders, A., Zuniga-Teran, A.A., Bakkensen, L., et al., 2024. Earth observation to address inequities in Post-flood recovery. Earth's Future 12 (2). https://doi.org/10.1029/2023ef003606.

Fussell, E., Sastry, N., Vanlandingham, M., 2010. Race, socioeconomic status, and return migration to New Orleans after hurricane Katrina. Popul. Environ. 31 (1–3), 20–42. https://doi.org/10.1007/s11111-009-0092-2.

Gould, R.K., Shrum, T.R., Ramirez Harrington, D., Iglesias, V., 2024. Experience with extreme weather events increases willingness-to-pay for climate mitigation policy. Glob. Environ. Chang. 85. https://doi.org/10.1016/j.gloenvcha.2023.102795.

Griggs, D., Stafford-Smith, M., Gaffney, O., Rockström, J., Öhman, M.C., Shyamsundar, P., et al., 2013. Sustainable development goals for people and planet. Nature 495 (7441), 305–307. https://www.nature.com/articles/495305a.pdf.

Hong, B., Bonczak, B.J., Gupta, A., Kontokosta, C.E., 2021. Measuring inequality in community resilience to natural disasters using large-scale mobility data. Nat. Commun. 12 (1), 1870. https://doi.org/10.1038/s41467-021-22160-w.

Howell, J., Elliott, J.R., 2019. Damages done: the longitudinal impacts of natural hazards on wealth inequality in the United States. Soc. Probl. 66 (3), 448–467. https://doi.org/10.1093/socpro/spy016.

Hsu, F., Zhizhin, M., Ghosh, T., Elvidge, C., Taneja, J., 2021. The annual cycling of nighttime lights in India. Remote Sens. 13 (6), 1199. https://doi.org/10.3390/rs13061199.

Hu, Y., Zhou, X., Yamazaki, D., Chen, J., 2024. A self-adjusting method to generate daily consistent nighttime light data for the detection of short-term rapid human activities. Remote Sens. Environ. 304. https://doi.org/10.1016/j.rse.2024.114077.

Imhoff, M.L., Lawrence, W.T., Stutzer, D.C., Elvidge, C.D., 1997. A technique for using composite DMSP/OLS city lights'' satellite data to map urban area. Remote Sens. Environ. 61 (3), 361–370.

Jia, M., Li, X., Gong, Y., Belabbes, S., Dell'Oro, L., 2023. Estimating natural disaster loss using improved daily night-time light data. Int. J. Appl. Earth Obs. Geoinf. 120. https://doi.org/10.1016/j.jag.2023.103359.

Jia, M., Zeng, H., Chen, Z., Wang, Z., Ren, C., Mao, D., et al., 2024. Nighttime light in China's coastal zone: the type classification approach using SDGSAT-1 glimmer imager. Remote Sens. Environ. 305. https://doi.org/10.1016/j.rse.2024.114104.

Jing, R., Heft-Neal, S., Chavas, D.R., Griswold, M., Wang, Z., Clark-Ginsberg, A., et al., 2024. Global population profile of tropical cyclone exposure from 2002 to 2019. Nature 626 (7999), 549–554. https://doi.org/10.1038/s41586-023-06963-z.

Kerber, S.W., Duncan, N.A., L'Her, G.F., Bazilian, M., Elvidge, C., Deinert, M.R., 2023. Tracking electricity losses and their perceived causes using nighttime light and social media. iScience 26 (12), 108381. https://doi.org/10.1016/j.isci.2023.108381.

Khan, S.I., Sarker, M.N.I., Huda, N., Nurullah, A., Zaman, M.R., 2018. Assessment of new urban poverty of vulnerable urban dwellers in the context of sub-urbanization in Bangladesh. J. Soc. Sci. Res. 4 (10), 184–193.

Kim, K., Bui, L., 2019. Learning from Hurricane Maria: island ports and supply chain resilience. In. J. Disaster Risk Reduct. 39. https://doi.org/10.1016/j.ijdrr.2019.101244.

Kyba, C., Garz, S., Kuechly, H., de Miguel, A., Zamorano, J., Fischer, J., Hölker, F., 2014. High-resolution imagery of Earth at night: new sources, opportunities and challenges. Remote Sens. 7 (1), 1–23. https://doi.org/10.3390/rs70100001.

Levin, N., 2023. Using night lights from space to assess areas impacted by the 2023 Turkey earthquake. Remote Sens. 15 (8). https://doi.org/10.3390/rs15082120.

Levin, N., Kyba, C.C.M., Zhang, Q., de Miguel, A.S., Roman, M.O., Li, X., et al., 2020. Remote sensing of night lights: A review and an outlook for the future. Remote Sens. Environ. 237. https://doi.org/10.1016/j.rse.2019.111443. Article 111443.

Li, X., Ma, R., Zhang, Q., Li, D., Liu, S., He, T., Zhao, L., 2019. Anisotropic characteristic of artificial light at night – systematic investigation with VIIRS DNB multi-temporal observations. Remote Sens. Environ. 233. https://doi.org/10.1016/j.rse.2019.111357.

Li, X., Levin, N., Xie, J., Li, D., 2020. Monitoring hourly night-time light by an unmanned aerial vehicle and its implications to satellite remote sensing. Remote Sens. Environ. 247. https://doi.org/10.1016/j.rse.2020.111942.

Li, T., Zhu, Z., Wang, Z., Román, M.O., Kalb, V.L., Zhao, Y., 2022. Continuous monitoring of nighttime light changes based on daily NASA's black marble product suite. Remote Sens. Environ. 282. https://doi.org/10.1016/j.rse.2022.113269.

Li, Q., Ramaswami, A., Lin, N., 2023. Exploring income and racial inequality in preparedness for hurricane Ida (2021): insights from digital footprint data. Environ. Res. Lett. 18 (12). https://doi.org/10.1088/1748-9326/ad08fa.

Lindell, M.K., Kang, J.E., Prater, C.S., 2011. The logistics of household hurricane evacuation. Nat. Hazards 58, 1093–1109.

Machlis, G.E., Roman, M.O., Pickett, S.T.A., 2022. A framework for research on recurrent acute disasters. Sci. Adv. 8 (10), eabk2458. https://doi.org/10.1126/sciadv.abk2458.

Markhvida, M., Walsh, B., Hallegatte, S., Baker, J., 2020. Quantification of disaster impacts through household well-being losses. Nat. Sustain. 3 (7), 538–547. https://doi.org/10.1038/s41893-020-0508-7.

Mu, T., Zheng, Q., He, S.Y., 2024. Robust disaster impact assessment with synthetic control modeling framework and daily nighttime light time series images. IEEE Trans. Geosci. Remote Sens. 1-1. https://doi.org/10.1109/TGRS.2024.3512549.

NOAA, 2024. U.S. Billion-Dollar Weather and Climate Disasters. Retrieved Feb.1, 2024 from. https://coast.noaa.gov/states/fast-facts/hurricane-costs.html.

Ohenhen, L.O., Shirzaei, M., Ojha, C., Sherpa, S.F., Nicholls, R.J., 2024. Disappearing cities on US coasts. Nature 627 (8002), 108–115. https://doi.org/10.1038/s41586-024-07038-3.

Oke, T.R., Mills, G., Christen, A., Voogt, J.A., 2017. Urban climates. Cambridge university press.

Park, S., Yao, T., Ukkusuri, S.V., 2024. Spatiotemporal heterogeneity reveals urban-rural differences in post-disaster recovery. npj Urban Sustain. 4 (1). https://doi.org/10.1038/s42949-023-00139-4.

Parks, R.M., Benavides, J., Anderson, G.B., Nethery, R.C., Navas-Acien, A., Dominici, F., et al., 2022. Association of tropical cyclones with county-level mortality in the US. JAMA 327 (10), 946–955.

Román, M.O., Wang, Z., Sun, Q., Kalb, V., Miller, S.D., Molthan, A., et al., 2018. NASA's Black Marble nighttime lights product suite. Remote Sens. Environ. 210, 113–143. https://doi.org/10.1016/j.rse.2018.03.017.

Román, M.O., Stokes, E.C., Shrestha, R., Wang, Z., Schultz, L., Carlo, E.A., et al., 2019. Satellite-based assessment of electricity restoration efforts in Puerto Rico after Hurricane Maria. PLoS One 14 (6), e0218883.

Ronco, M., Tarraga, J.M., Munoz, J., Piles, M., Marco, E.S., Wang, Q., et al., 2023. Exploring interactions between socioeconomic context and natural hazards on human population displacement. Nat. Commun. 14 (1), 8004. https://doi.org/10.1038/s41467-023-43809-8.

Sánchez de Miguel, A., Zamorano, J., Gómez Castaño, J., Pascual, S., 2014. Evolution of the energy consumed by street lighting in Spain estimated with DMSP-OLS data. J. Quant. Spectrosc. Radiat. Transf. 139, 109–117. https://doi.org/10.1016/j.jqsrt.2013.11.017.

Sanders, B.F., Schubert, J.E., Kahl, D.T., Mach, K.J., Brady, D., AghaKouchak, A., et al., 2022. Large and inequitable flood risks in Los Angeles, California. Nat. Sustain. 6 (1), 47–57. https://doi.org/10.1038/s41893-022-00977-7.

Sauer, J., Pallathadka, A., Ajibade, I., Berbés-Blázquez, M., Chang, H., Cook, E., et al., 2023. Relating social, ecological, and technological vulnerability to future flood exposure at two spatial scales in four U.S. cities. Sustain. Cities Soc. 99. https://doi.org/10.1016/j.scs.2023.104880.

Shi, K., Ma, J., Chen, Z., Cui, Y., Yu, B., 2023. Nighttime light remote sensing in characterizing urban spatial structure. Innovation Geosci. 1 (3). https://doi.org/10.59717/j.xinn-geo.2023.100043.

Smiley, K.T., Noy, I., Wehner, M.F., Frame, D., Sampson, C.C., Wing, O.E.J., 2022. Social inequalities in climate change-attributed impacts of Hurricane Harvey. Nat. Commun. 13 (1), 3418. https://doi.org/10.1038/s41467-022-31056-2.

Smith, A.B., Matthews, J.L., 2015. Quantifying uncertainty and variable sensitivity within the US billion-dollar weather and climate disaster cost estimates. Nat. Hazards 77, 1829–1851.

Sotolongo, M., Kuhl, L., Baker, S.H., 2021. Using environmental justice to inform disaster recovery: vulnerability and electricity restoration in Puerto Rico. Environ. Sci. Pol. 122, 59–71.

Stokes, E.C., Seto, K.C., 2019. Characterizing urban infrastructural transitions for the Sustainable Development Goals using multi-temporal land, population, and nighttime light data. Remote Sens. Environ. 234. https://doi.org/10.1016/j.rse.2019.111430.

Tan, X., Zhu, X., Chen, J., Chen, R., 2022. Modeling the direction and magnitude of angular effects in nighttime light remote sensing. Remote Sens. Environ. 269. https://doi.org/10.1016/j.rse.2021.112834.

Thonis, A., Stansfield, A., Akcakaya, H.R., 2024. Unravelling the role of tropical cyclones in shaping present species distributions. Glob. Chang. Biol. 30 (3), e17232. https://doi.org/10.1111/gcb.17232.

U.S. DOE, 2018. Hurricanes Nate, Maria, Irma, and Harvey Situation Reports. Retrieved 2024-04-01 from. https://www.energy.gov/ceser/articles/hurricanes-nate-maria-irma-and-harvey-situation-reports.

UN, 2023. A Review of Gender and the Sendai Framework. https://www.undrr.org/publication/review-gender-and-sendai-framework.

United States Census Bureau, 2023. County Population Totals: 2020-2023. http://www.census.gov/data/tables/time-series/demo/popest/2020s-counties-total.html.

Vestby, J., Schutte, S., Tollefsen, A.F., Buhaug, H., 2024. Societal determinants of flood-induced displacement. Proc. Natl. Acad. Sci. USA 121 (3), e2206188120. https://doi.org/10.1073/pnas.2206188120.

Wang, Z., Román, M.O., Kalb, V.L., Miller, S.D., Zhang, J., Shrestha, R.M., 2021. Quantifying uncertainties in nighttime light retrievals from Suomi-NPP and NOAA-20 VIIRS Day/Night Band data. Remote Sens. Environ. 263, 112557. https://doi.org/10.1016/j.rse.2021.112557.

Wehner, M.F., Kossin, J.P., 2024. The growing inadequacy of an open-ended Saffir-Simpson hurricane wind scale in a warming world. Proc. Natl. Acad. Sci. USA 121 (7), e2308901121. https://doi.org/10.1073/pnas.2308901121.

Wing, O.E.J., Lehman, W., Bates, P.D., Sampson, C.C., Quinn, N., Smith, A., M.,…Kousky, C., 2022. Inequitable patterns of US flood risk in the Anthropocene. Nat. Clim. Chang. 12 (2), 156–162. https://doi.org/10.1038/s41558-021-01265-6.

Wu, Y., Li, X., 2024. Exploring the drivers of variations in daily nighttime light time series from the perspective of periodic factors. IEEE Geosci. Remote Sens. Lett. 21, 1–5. https://doi.org/10.1109/lgrs.2024.3358856.

Xi, D., Lin, N., Gori, A., 2023. Increasing sequential tropical cyclone hazards along the US east and gulf coasts. Nat. Clim. Chang. 13 (3), 258–265. https://doi.org/10.1038/s41558-023-01595-7.

Xu, J., Qiang, Y., Cai, H., Zou, L., 2023. Power outage and environmental justice in winter storm Uri: an analytical workflow based on nighttime light remote sensing. Int. J. Digital Earth 16 (1), 2259–2278. https://doi.org/10.1080/17538947.2023.2224087.

Zhang, D., Huang, H., Roy, N., Roozbahani, M.M., Frost, J.D., 2023. Black marble nighttime light data for disaster damage assessment. Remote Sens. 15 (17). https://doi.org/10.3390/rs15174257.

Zhao, K., Wulder, M.A., Hu, T., Bright, R., Wu, Q., et al., 2019. Detecting change-point, trend, and seasonality in satellite time series data to track abrupt changes and nonlinear dynamics: A Bayesian ensemble algorithm. Remote Sens. Environ. 232. https://doi.org/10.1016/j.rse.2019.04.034.

Zheng, Q., Weng, Q., Wang, K., 2021. Characterizing urban land changes of 30 global megacities using nighttime light time series stacks. ISPRS J. Photogramm. Remote Sens. 173, 10–23. https://doi.org/10.1016/j.isprsjprs.2021.01.002.

Zheng, Q., Weng, Q., Zhou, Y., Dong, B., 2022a. Impact of temporal compositing on nighttime light data and its applications. Remote Sens. Environ. 274, 113016. https://doi.org/10.1016/j.rse.2022.113016.

Zheng, Z., Wu, Z., Cao, Z., Zhang, Q., Chen, Y., et al., 2022b. Estimates of power shortages and affected populations during the initial period of the Ukrainian-Russian conflict. Remote Sens. 14 (19). https://doi.org/10.3390/rs14194793.

Zheng, Q., Seto, K.C., Zhou, Y., You, S., Weng, Q., 2023. Nighttime light remote sensing for urban applications: Progress, challenges, and prospects. ISPRS J. Photogramm. Remote Sens. 202, 125–141. https://doi.org/10.1016/j.isprsjprs.2023.05.028.